Check for updates

Electrochemical sensing of Hg(II) in chicken liver and snail shell extract samples using novel modified SDA/MWCNT electrodes

Jayagopi Gayathri,*[a] A. Roniboss,[a] Sivakumar Sivalingam [ID] *[a] and Kumar Sangeetha Selvan[b]

Heavy metal ions (Hg(II)) were detected in fresh chicken liver and snail shell extract samples using novel synthesised SDA/MWCNT-modified electrodes. The synthesized N,N'-bis(salicylaldehyde)-1,2-diaminobenzene (SDA) ligand was characterized *via* FT-IR, ^{1}H-NMR, and ^{13}C-NMR spectroscopy. The hydroxyl and imine functional groups present in SDA act as active sites and bind to the MWCNT surface. The surface morphology of the modified SDA/MWCNT electrode exhibited a star-like crystal structure and the preconcentration of Hg(II)-SDA/MWCNTs lead to a crystal cloud structure, as characterized by SEM with EDX. The enhancement of current and conductance of the SDA/MWCNT- and MWCNT-modified electrode was investigated by cyclic voltammetry (CV) and electrochemical impedance spectroscopy (EIS). The conductance (σ) values for the MWCNT- and SDA/MWCNT-modified electrodes are 234.1×10^{-5} S cm^{-1} and 358.4×10^{-5} S cm^{-1}, respectively, as determined by electrochemical impedance spectroscopy. Consequently, an electrochemical sensor with outstanding performance in terms of reproducibility, stability and anti-interference ability was fabricated. The stripping analysis of Hg(II) was performed using square wave anodic stripping voltammetry (SWASV) and cyclic voltammetry (CV). Using SWASV, a linear range of Hg(II) response was found to be 1.3 to 158 μg L^{-1}, and the limit of detection (LOD) was 0.24 μg L^{-1}. Finally, the results of the recovered value of Hg(II) in freshly prepared chicken liver and snail shell extract samples by SWASV were compared with the atomic absorption spectroscopy (AAS) results.

1. Introduction

Mercury is a naturally occurring heavy metal that is widely dispersed throughout the environment (air, water, and soil). The Environmental Protection Agency (EPA) classifies it as a worldwide contaminant and a very harmful element owing to its severe immunotoxic, neurotoxic, and genotoxic properties.[1–3] The toxic heavy metals mercury (Hg(II)) and cadmium (Cd(II)) in their +2 oxidation state can seriously harm the human central nervous system (CNS), skin, muscle tissue (Hg(II)), bones, blood plasma, cardiovascular system (Cd(II)), renal system, and gastrointestinal tract.[4–6] According to the United States (US) Agency for Toxic Substances and Disease Registry (ATSDR).[7] For instance, mercury has widespread industrial applications like lamps, batteries, thermometers, and electrolytic manufacture in chlorine and sodium hydroxide.[8,9] At an equivalent time, the applicability of lead exposure is automobile exhaust gas, industrial emissions and battery production.[10,11] Heavy metal ions are present in groundwater is usually not decomposed whereas they are moving but can only be converted into other forms or occurrence modes.[12,13] To safeguard public health, the concentration of mercuric ions in drinking water must not exceed the threshold limit of 4.7 nM.[14] Therefore, precise identification and remediation of water toxins are extremely important for ensuring public safety.[15] Mercury is the third most deadly element for humans. Mercury is extensively used in industrial applications such as in the manufacturing of thermometers, batteries, and lamps.

The monitoring of heavy metal ions present in environmental quality, which is currently under pressure considering the growing pollution and the increasing industrial, agricultural, and residential activities, depends heavily on the determination and effective removal of heavy metal ions from aquatic sources.[16–19] Therefore, developing sensitive and repeatable analytical methods for the detection of these heavy metals at low levels is essential.

Inductively coupled plasma-mass spectrometry (ICP-MS),[22,23] atomic fluorescence spectroscopy (AFS),[24] coulometry,[20] atomic absorption spectroscopy (AAS),[21] and other conventional analytical techniques are widely applied for mercury detection

[a]Department of Chemistry, VelTech Rangarajan Dr Sagunthala R & D Institute of Science and Technology, Avadi, Chennai, Tamil Nadu 600 062, India. E-mail: drsivakumars@veltech.edu.in

[b]Department of Chemistry, Anna Adarsh College for Women, Anna Nagar, Chennai, Tamil Nadu 600040, India

to determine the amount of Hg(II) in food and water samples. These methods generally show good and consistent sensitivity toward Hg(II). The determination of Hg(II) more practical and affordable for alternative analytical techniques due to the drawbacks of the expensive, time-consuming, and expert requirements. In order to detect trace levels of Hg(II), the electrochemical analytical approach is currently commonly used owing to its high sensitivity and stability, low cost, and ease of operation.[25–29]

SWASV is a well-known sensitive approach among the many electrochemical sensing methods due to its quick analysis speed, simplicity of usage, and utilization of affordable and portable equipment.[30–34]

In electrochemical analysis, improved electrodes based on nanostructured materials have gained tremendous interest[35,36] and have been researched to provide sensitive Hg(II) detection. Carbon nanomaterials that have been heavily coated on electrode surfaces to improve stability, conductivity, and sensitivity with low detection limits for suggested methods include metal nanoparticles,[39] graphene materials,[38] and multiwalled carbon nanotubes (MWCNTs).[37] Particularly in the field of sensing, MWCNTs have grown. The use of MWCNTs suggests low potential current, strong electronic conductivity, surface functionalization capability, and charge transfer reactions.[40] Due to the characteristics including poor dispersion of metal nanoparticles and reduced active site availability, MWCNT utility in anodic stripping voltammetric measurements is still limited. To overcome these issues, the surface of multiwalled carbon nanotubes should be modified appropriately.[40] Generally, the mercury-based electrode is used for the stripping voltammetric detection of metal ions. The disadvantage of mercury-based electrodes is that they cannot be used for the determination of mercury ions. In light of these considerations, we flexibly synthesized N,N'-bis(salicylaldehyde)-1,2-diaminobenzene Schiff base (SDA) ligand using 1,2-diaminobenzene and salicylaldehyde by a condensation method.[41] Next, using the square wave anodic stripping voltammetry method, we modified a paraffin wax-impregnated

graphite electrode (PGE) using SDA/MWCNT materials to detect Hg(II) in freshwater snail shell and chicken liver samples. Scheme 1 shows the structure of N,N'-bis(salicylaldehyde)-1,2-diaminobenzene (SDA). In the pre-concentration stage, the diamine with *ortho* hydroxyl groups present in SDA could form complexes with Hg(II).

The novelty of this work is that the SDA/MWCNTs were characterized and applied for the detection of Hg(II) in freshly prepared chicken liver and snail shell extracts. The SDA ligand coated on the MWCNT electrode surface, the conductance of SDA/MWCNTs and MWCNTs have been characterised by cyclic voltammetry (CV) and electrochemical impedance spectroscopy (EIS). The Hg(II)-SDA/MWCNT was confirmed by SEM with EDX, cyclic voltammetry and square wave anodic stripping voltammetry. To the best of our knowledge, the novel proposed electrode is used for the sensing of Hg(II), even at very low concentrations with a good recovery of 99.4 to 102.3%. The recorded sample values of square wave anodic stripping voltammetry are correlated with atomic absorption spectroscopy.

## 2. Experimental

2.1. Chemicals and apparatus

Multiwalled carbon nanotubes (with a particle size of 110 nm with purity greater than 90%), salicylaldehyde, 1,2-diaminobenzene, acetate salt of mercury, sodium and acetic acid were purchased from Merck Pvt. Ltd India. All reagents used were of AnalaR grade. Sodium nitrate solutions (0.1 M) with a pH ranging from 4.0 to 6.5 were prepared with sodium nitrate, sodium hydroxide and hydrochloric acid. All the solutions were prepared using DD water. The coated electrodes were characterised by scanning electron microscopy (SEM Hitachi Sv-6600 microscope, Japan). The voltammetric analysis was performed using CHI-660-B and IviumSoft electrochemical workstations with a three-electrode set-up comprising platinum as the counter electrode, a saturated KCl calomel electrode as the reference electrode and MWCNTs and SDA/MWCNTs as the working electrode. The pH measurements were made using a digital pH meter (Digisun electronic system). All the analyses were performed at ambient temperature. Chicken liver and snail shells were purchased from Poonamallee (avadi), Tamil Nadu, India.

2.2. Synthesis of SDA

First, 1,2-diaminobenzene (5 mmol) and salicylaldehyde (13.10 mmol) were dissolved and stirred in methanol for 30 min to afford a new Schiff base N,N'-bis(salicylaldehyde)-1,2-diaminobenzene (SDA), which was washed, repeatedly dried and then recrystallized using methanol and a high-quality product (∼70–75%) was obtained (Scheme 2).

2.3. Fabrication of SDA/MWCNTs

A paraffin wax-impregnated graphite electrode (PGE) was prepared following the procedure reported in the literature.[42] An SDA/MWCNT-modified electrode was prepared: initially, MWCNTs (0.1 mg) were dispersed in 1 mL of ethanol by ultrasonication, for 45 min, and then 10 μL of dispersed solution of
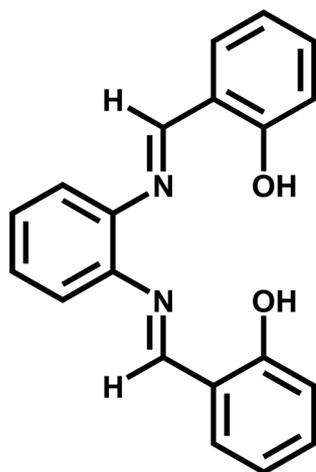
Scheme 1 Structure of N,N'-bis(salicylaldehyde)-1,2-diaminobenzene (SDA).

N,N'-bis(salicylaldehyde)-1,2-diaminobenzene (SDA)
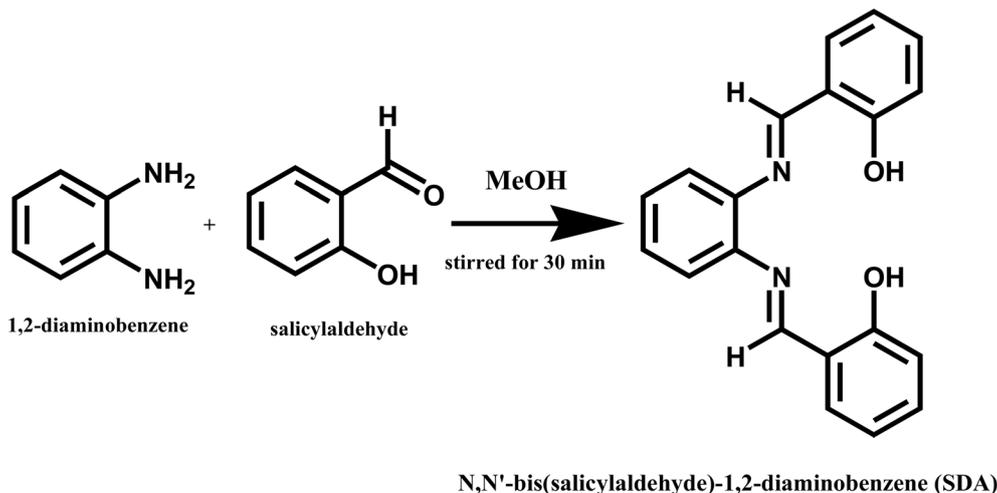
Scheme 2 Synthesis of *N,N'*-bis(salicylaldehyde)-1,2-diaminobenzene (SDA).

multiwalled carbon nanotubes (MWCNTs) was coated onto the polished PGE. Then, 1 mM synthesised SDA ligand (10 μL) added into an acetonitrile solution was mantled onto the modified MWCNT electrode and then allowed to dry under ambient conditions, and an SDA/MWCNT-modified electrode was obtained.

2.4. Standard solution method

First, 1 mM Hg(II) as a stock solution was prepared by adding NaNO$_3$ with pH 5.0. Then, 0.1 mM solutions of Hg(II) in pH 5.0 NaNO$_3$ were made as the stock solution by sequential dilution. Following that, 0.06 μL of Hg(II) was spiked in a known amount of NaNO$_3$ solutions.

2.5. Preparation of freshly prepared chicken liver and snail shell extract samples
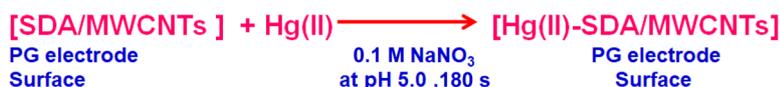
Hg(II) analysis was performed according to an earlier published method (22–23). Sample-A (chicken liver extract sample) was chopped, homogenized thoroughly using a stainless steel knife

and sample-A and sample-B were considerably washed with DD water subsequently and kept at 100 °C in an oven for drying, and made into a powder sample. Both the samples, sample-A (chicken liver extract) and sample-B (snail shells extract) were dissolved in 0.1 mM of Hg(II) and made as stocked solutions for further analyses. Hence, these samples are used for the measurement of Hg(II) by SWASV and the resultant values are compared with AAS.
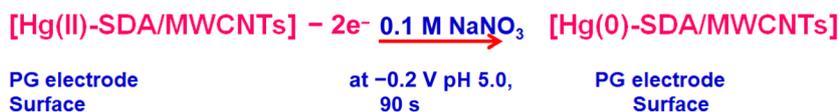
2.6. Stripping measurement of Hg(II) on SDA/MWCNTs

The stripping analysis of Hg(II) was performed on the SDA/MWCNT-modified electrode by dipping the SDA/MWCNT electrode in 0.1 M NaNO$_3$ (pH 5.0) with 30 μg per L preconcentrated Hg(II) for 180 s under mechanically constant stirring conditions. The electrode was changed into the freshly prepared solution of 0.1 M NaNO$_3$. Hg(II) was reduced at −0.2 V for 90 s on the surface of the electrode. Reduction of Hg(II) to Hg(0) on the electrode surface were anodic oxidisation take place from the potential range between −0.2 and 0.6 V. The steps involved are explained as follows:
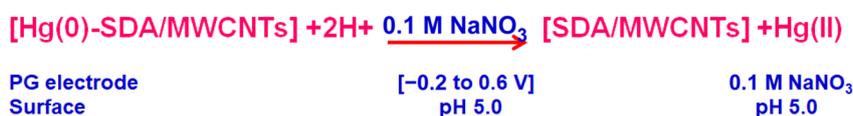
1. Preconcentration step: (Metal complex)

[SDA/MWCNTs] + Hg(II) ⟶ [Hg(II)-SDA/MWCNTs]
PG electrode · · · · · 0.1 M NaNO$_3$ · · · · · PG electrode
Surface · · · · · at pH 5.0 ,180 s · · · · · Surface

2. Reduction step: (Hg(II) ⟶ Hg(0))

[Hg(II)-SDA/MWCNTs] − 2e$^-$ $\xrightarrow{\text{0.1 M NaNO}_3}$ [Hg(0)-SDA/MWCNTs]
PG electrode · · · · · at −0.2 V pH 5.0, · · · · · PG electrode
Surface · · · · · 90 s · · · · · Surface

3. Stripping Step: (M^0 ⟶ M^{2+})

[Hg(0)-SDA/MWCNTs] +2H+ $\xrightarrow{\text{0.1 M NaNO}_3}$ [SDA/MWCNTs] +Hg(II)
PG electrode · · · · · [−0.2 to 0.6 V] · · · · · 0.1 M NaNO$_3$
Surface · · · · · pH 5.0 · · · · · pH 5.0

3. Results and discussion

3.1. Characterization of N,N′-bis(salicylaldehyde)-1,2-diaminobenzene (SDA)

3.1.1. Fourier transform infrared (FT-IR) spectroscopy analysis. The synthesised SDA ligand was characterized by FT-IR spectroscopy. In the spectrum, ligand was studied in the range of 600 to 4000 cm^{-1} to verify the presence of phenolic hydroxyl and imine nitrogen groups. Fig. 1 shows the absorption of strong intense peak at 3414 cm^{-1} due to the presence of hydroxyl groups. The absorption peaks at 1614 cm^{-1} and 1290 cm^{-1} indicates the presence of (C=N) and (C=O) groups respectively. The spectra confirm the presence of hydroxyl (OH) groups and imino nitrogen (C=N) groups in the synthesized SDA ligand, as reported earlier.[40]

3.2. Nuclear magnetic resonance spectroscopy (^{1}H-NMR and ^{13}C-NMR) analysis

^{1}H-NMR and ^{13}C-NMR spectroscopies were used to determine the chemical structure of the synthesized SDA ligand, as illustrated in Fig. 2 and 3, respectively.[40] ^{1}H-NMR (300 MHz, CDCl$_3$): 13.078 (s, 2H), 8.628 (s, 2H), 7.389–7.313 (m, J = 12 Hz, 5H), 7.253–7.213 (m, J = 12 Hz, 2H), 7.055–6.892 (m, J = 12 Hz, 4H). ^{13}C-NMR (300 MHz, CDCl$_3$): 117.56, 119.00, 119.24, 119.74, 127.72, 132.35, 133.40, 142.56, 161.35, 163.73.

3.3. Morphological analysis of SDA/MWCNTs

SEM and EDX were performed on the surface structure of the PGE, MWCNTs, SDA/MWCNTs, Hg(II)-MWCNTs, and Hg(II)-SDA/MWCNT-modified electrodes, as shown in Fig. 4. PGE shows a polished surface (A) and EDX image (F) indicates the presence of a carbon peak. The MWCNT electrode showed a rod-like structure (B) and EDX spectra show carbon and oxygen peaks (G). Due to the presence of mercury ions in the MWCNT electrode, it exhibited a semi-rod-like morphology (C) and the EDX image authenticated the presence of carbon,

oxygen and mercury (H). The SDA/MWCNT electrode in the SEM image exhibited a star-like crystal structure (D) and the EDX image manifested the presence of carbon, oxygen and nitrogen(I). Owing to the preconcentration of the Hg(II)-SDA/MWCNT complex, it showed a crystal cloud structure (E) and EDX results indicated the presence of mercury, carbon, oxygen and nitrogen peaks (J). The above-mentioned results indicated the mercury ion interaction with the SDA ligand, which contains hetero atoms such as nitrogen and oxygen groups, it has lone pair of electrons which coordinate with mercury ions to form a more stable complex [Hg(II)-SDA/MWCNTs] called the modified electrode.

3.4. Electrochemical characterization of the SDA/MWCNTs

The electrochemical behaviours of the modified electrodes (SDA/MWCNTs and MWCNTs) were investigated by cyclic voltammogram (CV) utilising [Fe(CN)$_6$]$^{3-/4-}$ which involves a redox reaction. The CV of the bare electrode (PGE) and SDA/MWCNTs was observed in the presence of 1 mmol of ferro/ferricyanide containing 0.1 M KCl at a scan rate of 50 mV, as shown in Fig. 5A. In bare electrode (PGE), the CV data exhibit least electrochemical behaviour with high capacitive loop current, increase peak to peak potential separation of ΔE_p 267 mv it shows broader wave shape curve. In the case of MWCNTs and SDA/MWCNT-modified electrodes, the ΔE_p values were estimated to be 220 mV and 180 mV respectively, which are provided in Table 2. The bare PGE and MWCNT-modified electrode showed a higher ΔE_p value correlated with the SDA/MWCNT-modified electrode. The higher peak separation was considered to lower the electrical conductivity. Moreover, modifying the bare PGE with MWCNTs has enhanced the peak current I_{pa} at MWCNTs from 40 μA to 75 μA. Meanwhile, a sharp intense peak with the increase in peak current (205 μA) was noticed for SDA/MWCNTs. A decrease in the ΔE_p value with the increase in the peak current value of SDA/MWCNTs could be attributed to the addition of MWCNTs owing to the enhanced electron transfer behaviour as well as the surface area. Therefore, it can be concluded from the results that SDA/MWCNTs have superior electro catalytic properties towards the catalysis of ferri–ferrocyanide redox probes.

The electro active surface area of PGE, SDA/MWCNT, and MWCNT electrodes was examined using the Randles-Sevcik eqn (1) as follows:

$$I_p = (2.69 \times 10^5)n^{3/2}ACD^{1/2}\nu^{1/2} \tag{1}$$

where A, D, C and ν are the area of the electrode (cm^2), diffusion coefficient of the material (cm^2 s^{-1}), concentration of the molecule in the bulk solution (mol cm^{-3}) and scan rate (ν/s) for using a 1 mM ferro/ferricyanide complex containing 0.1 M KCl. From the above-mentioned equations, the electro active surface area of PGE was estimated to be 0.013 cm^2, for the MWCNT electrode it was observed at 0.080 cm^2 and for the SDA/MWCNT-modified electrode it was 0.153 cm^2.

3.4.1. Studies of electrochemical impedance spectroscopy. The electrochemical impedance spectroscopy (EIS) spectra were recorded in 1 mM [Fe (CN)$_6$]$^{3-/4-}$ complex containing a 0.1 M
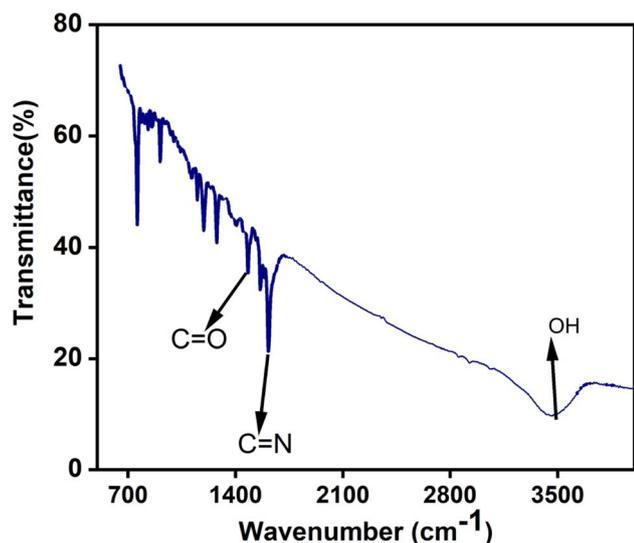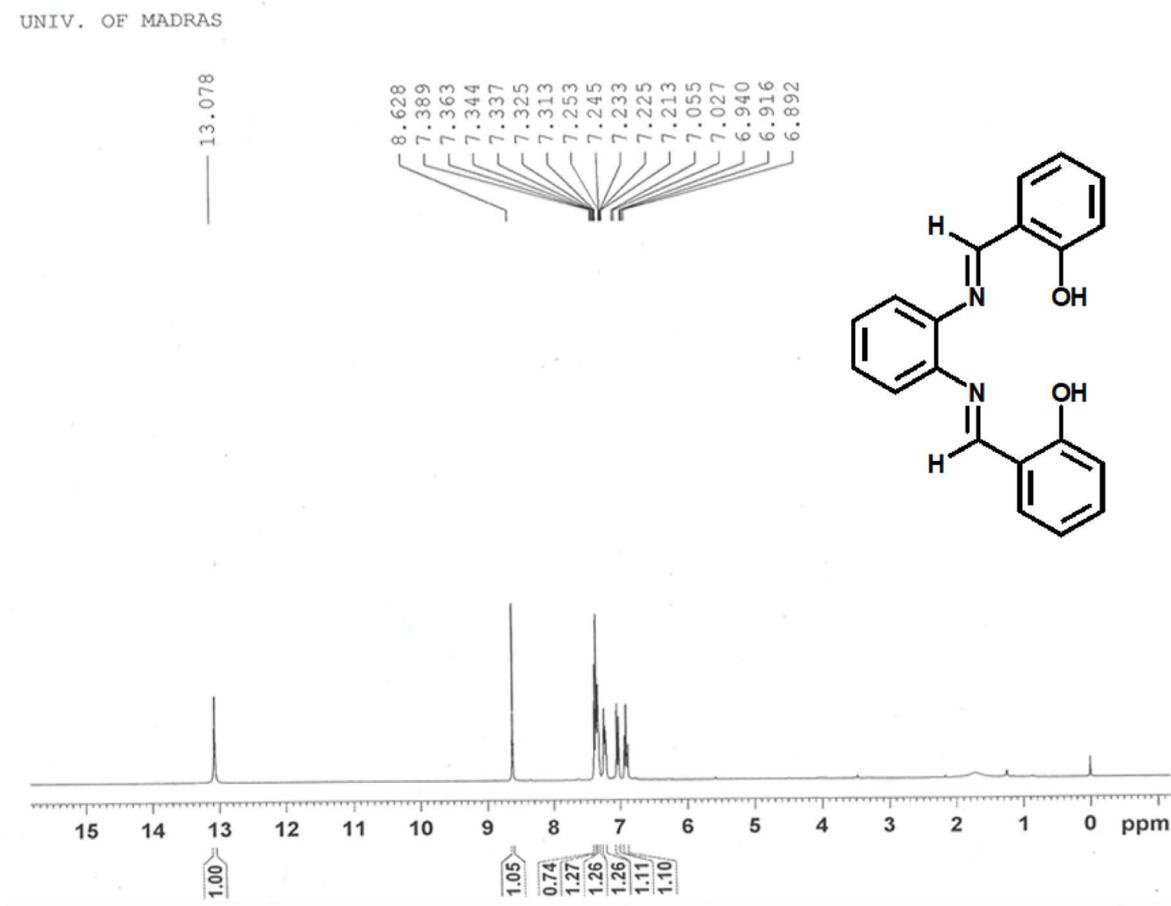

Fig. 1 FT-IR spectra of SDA.

UNIV. OF MADRAS

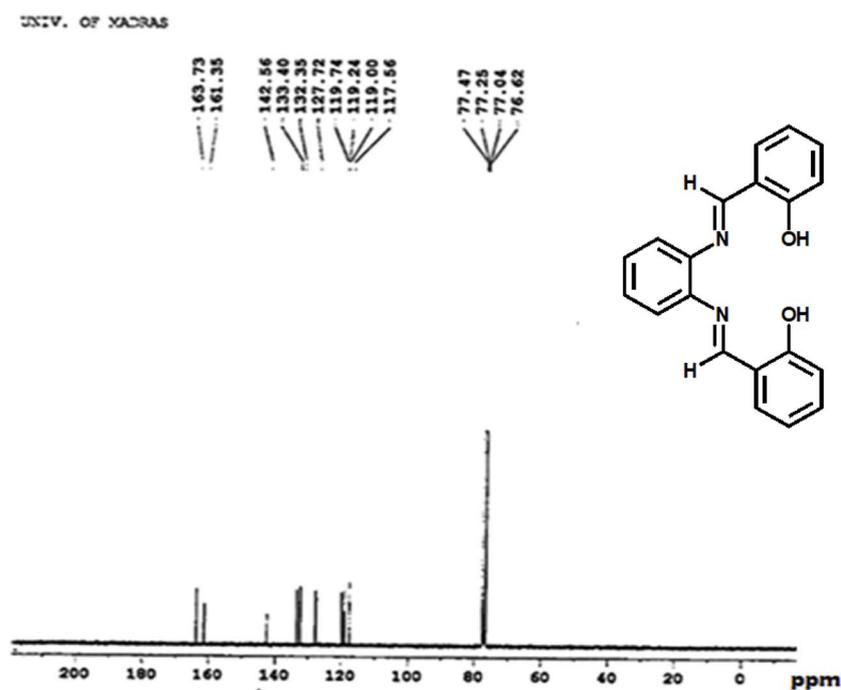**Fig. 2** ¹H-NMR spectra of *N,N′*-bis(salicylaldehyde)-1,2-diaminobenzene (SDA).

UNIV. OF MADRAS

Fig. 3 ¹³C-NMR spectra of *N,N′*-bis(salicylaldehyde)-1,2-diaminobenzene (SDA).

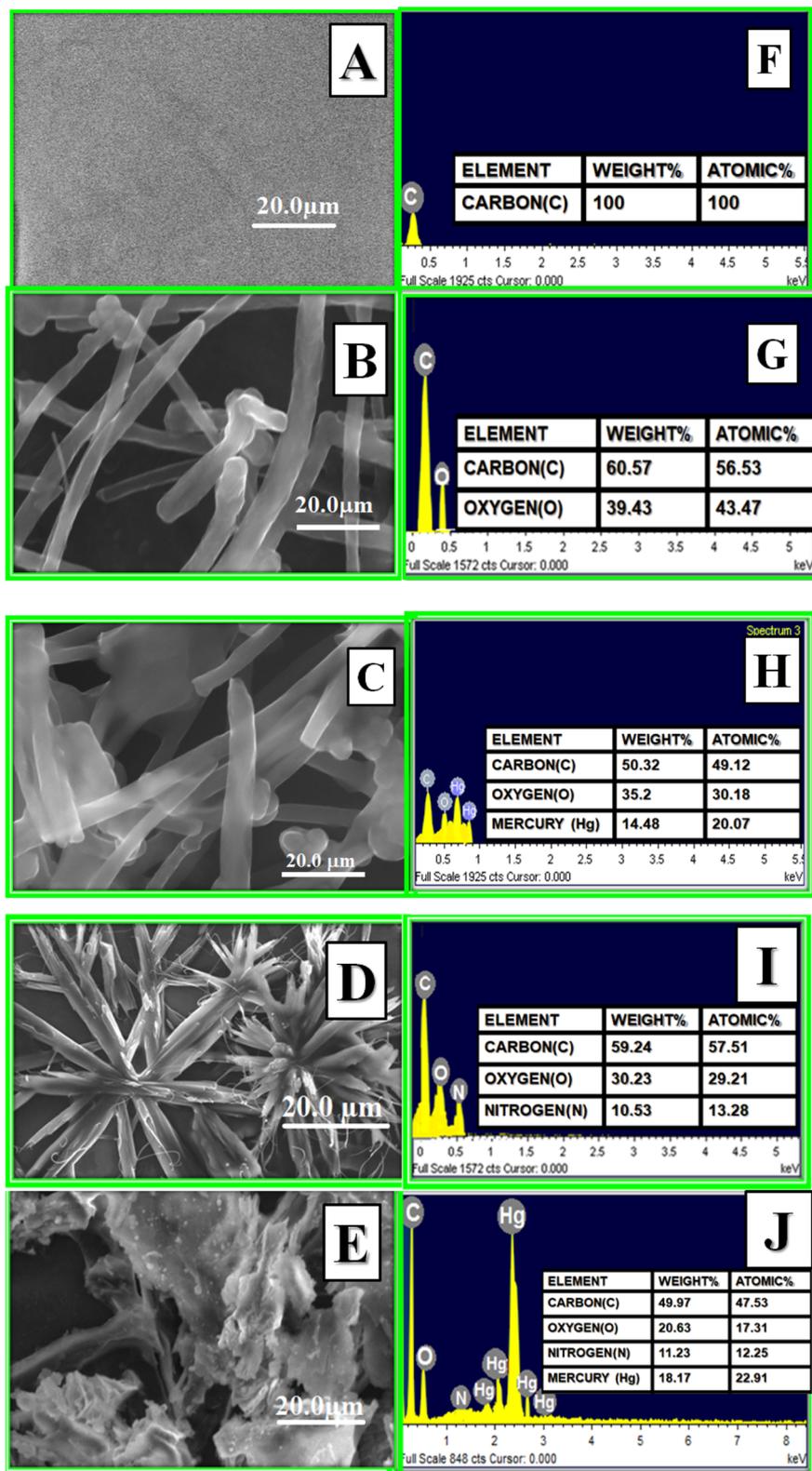© 2024 The Author(s). Published by the Royal Society of Chemistry

Fig. 4 Surface morphology of the proposed electrodes: (A) PGE with EDX image (F), (B) MWCNTs with EDX image (G), (C) Hg(II)-MWCNTs with EDX image (H), (D) SDA/MWCNTs with EDX image (I) and (E) Hg(II)-SDA/MWCNTs with EDX image (J).
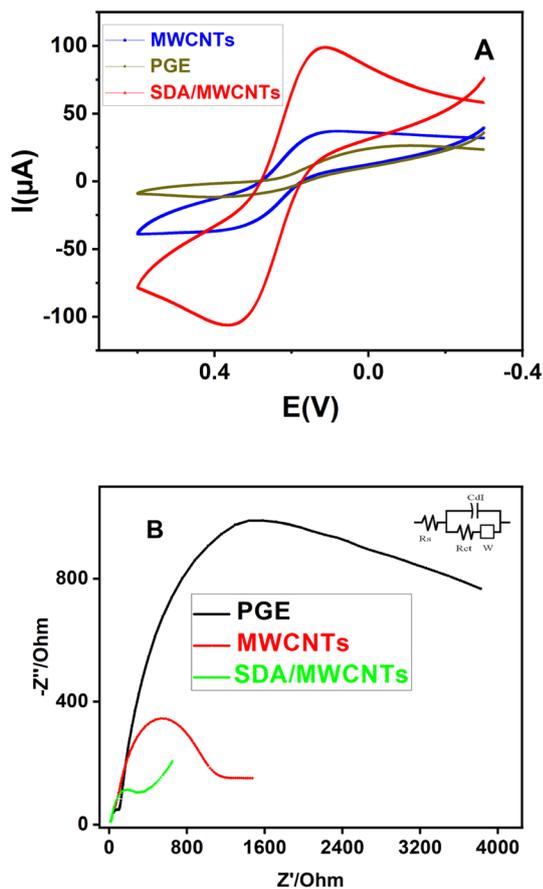
Fig. 5 Comparison of PGE, MWCNT and SDA/MWCNT electrodes using electrochemical studies by cyclic voltammogram (A) and impedance (B) in a 1 mM ferro/ferricyanide complex.

KCl solution over frequencies ranging between 0.1 Hz and 1.0 MHz, and are shown in Fig. 5B. In the Nyquist plot, the semicircle part indicates the charge transfer resistance (R_{ct}) at higher frequencies, whereas the lower frequencies at a linear part show a diffusion limited process. Further, the solution resistance (R_s) for PGE, MWCNTs and SDA/MWCNT-modified electrodes is 54.3, 30.16 Ω and 24.2 Ω. The R_{ct} value for the PGE bare electrode was observed at 7370 Ω, for the MWCNT electrode to be 986.2 Ω and for the SDA/MWCNT-modified electrode to be 200.4 Ω. The schematic of the modified Randle's equivalent circuit for the SDA/MWCNT-modified electrode is shown in the inset of Fig. 5B. From the circuit, R_{ct} is the charge transfer, R_s is the solution resistance, W is the Warburg resistance and C_{dl} is the capacitance. It is evident that R_{ct} of the SDA/MWCNT-modified electrode is smaller than that of the MWCNT electrode, further confirming the better conductivity of the SDA/MWCNT-modified electrode.

The electrode conductance (σ) for MWCNT-modified and SDA/MWCNT-modified electrodes was calculated using eqn (2):

$$\sigma = \frac{l}{A} \times \frac{1}{R} \tag{2}$$

where l is the length, A is the surface area and R is the resistance of the electrodes (MWCNTs and SDA/MWCNT-modified working electrodes). By using eqn (2), the electrode conductivity for PGE was evaluated to be 167×10^{-5} S cm^{-1}, for the

MWCNTs to be 234.1×10^{-5} S cm^{-1} and for the SDA/MWCNT-modified electrode to be 408.1×10^{-5} S cm^{-1}. The calculated data are shown in Table 2. Hence, the SDA/MWCNT-modified electrode has a higher conductivity than that of the MWCNTs. Therefore, the result reveals that the SDA/MWCNTs exhibited higher conductivity and fast electron transfer kinetics. Therefore, the purposed method is appropriate to determine Hg(ii) by stripping anodic voltammetry.

3.5. Electrochemical quantification of Hg(ii)

The determination of Hg(ii) on SDA/MWCNTs and MWCNT-modified electrodes by cyclic voltammetry is shown in Fig. 6. The modified electrodes were dipped in 0.1 M NaNO$_3$ containing 35 μg L^{-1} of Hg(ii) for the preconcentration method at 180 s. Then, the modified electrodes were cleaned and moved into a fresh electrolyte of 0.1 M NaNO$_3$ solution. Therefore, the cyclic voltammetric of preconcentrated of Hg(ii)-SDA/MWCNTs is enhanced well redox peak correlate with Hg(ii)-MWCNTs. In Fig. 6, the well redox peak for Hg(ii) is shown, which confirmed the selectivity of metal ions.
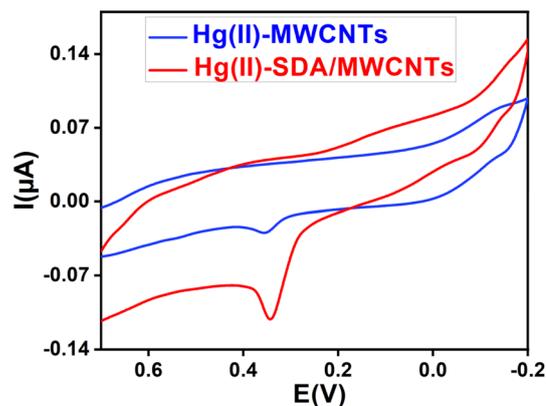

Fig. 6 Detection of Hg(ii) through cyclic voltammograms using MWCNTs and SDA/MWCNTs in 0.1 M NaNO$_3$ (pH 5.0) at 35 μg L^{-1} Hg(ii); scan rate: 50 mV s^{-1}.

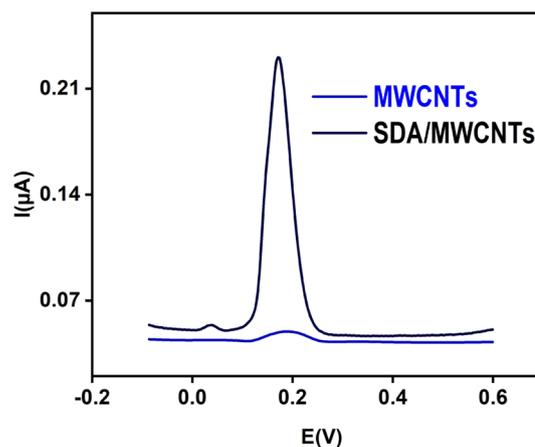**Fig. 7** Analysis of Hg(ii) using square wave anodic stripping voltammetry of MWCNTs and SDA/MWCNTs in 0.1 M NaNO$_3$ (pH 5.0) containing 20 μg L^{-1} Hg(ii); scan rate: 50 mV s^{-1}.

Using square wave anodic stripping voltammetry (SWASV), the modified electrodes of MWCNTs and SDA/MWCNTs for the analysis of Hg(II) were investigated, as shown in Fig. 7. A 20 µg L^{-1} Hg(II) solution was preconcentrated by dipping the electrode into a 0.1 M NaNO$_3$ solution (pH 5.0) under stirring for 180 s. Afterwards, the metal was reduced at a potential of -0.2 V for 90 s. Subsequently, by applying a positive direction potential of -0.2 to 0.6 V, the metal was stripped from the electrode into the solution. The result shows that, SDA/MWCNTs modified electrode the stripping peak current for Hg(II) was increase compared to MWCNTs electrode. Consequently, it was inferred that the SDA ligand present on the surface of the MWCNT electrode get absorbed with metal ions in the preconcentrated medium (the SDA ligand contains two nitrogen groups and hydroxyl group coordinated with metal ions) and the MWCNT electrode used for the stability of the electrode. Hence, the SDA/MWCNTs enhanced the sensitivity of Hg(II).

3.5.1. Effect of supporting medium, pH and preconcentration time. For the stripping voltammetric detection of Hg(II), the effect of parameters such as supporting electrolytes, pH and preconcentration time were studied, and the obtained results are presented in Fig. 8.

The stripping voltammogram for Hg(II) obtained in 0.1 M solutions of various media, such as acetate buffer, KNO$_3$, NH$_4$NO$_3$, and NaNO$_3$, was studied. The results of different electrolytes for 55 µg L^{-1} of Hg(II) were obtained, and are shown in Fig. 8A. The higher stripping current response in a NaNO$_3$ medium was established. Thus, the subsequent measurements in a 0.1 M NaNO$_3$ medium were done for the determination of Hg(II).

The effect of pH on the preconcentration of 55 µg per L Hg(II) on the anodic stripping current in 0.1 M NaNO$_3$ was studied. The variations in the stripping current for Hg(II) were studied at pH 4.0 to 6.5, and the results are given in Fig. 8B. It was
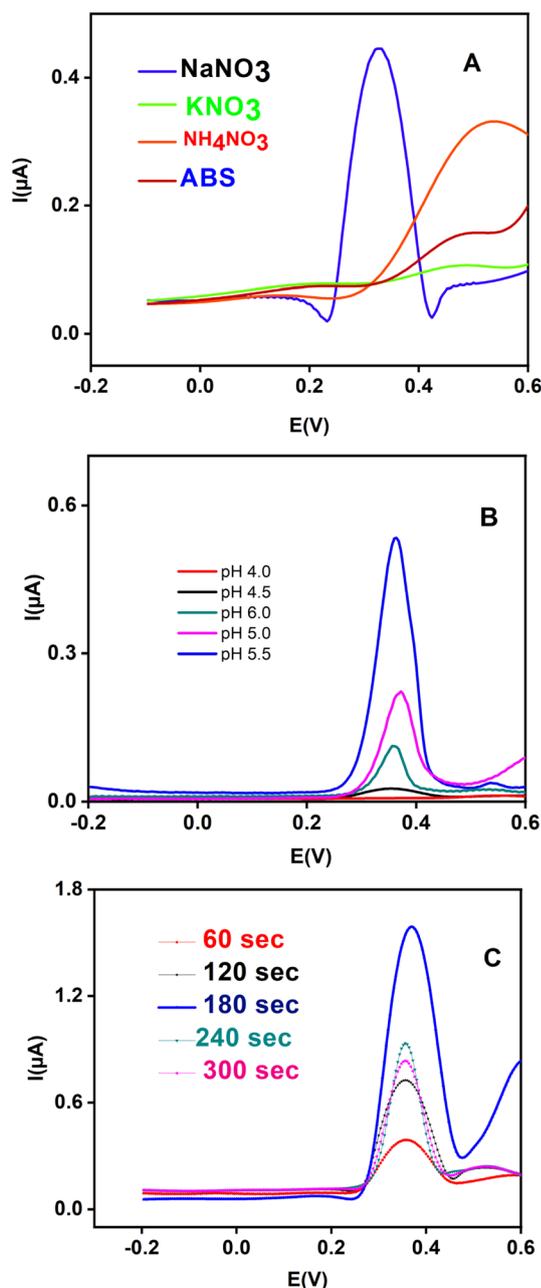
Fig. 8 Determination of Hg(II) *via* square wave anodic stripping voltammetry using SDA/MWCNTs at 55 µg per L Hg(II) in (A) different electrolytes, (B) pH media, and (C) preconcentration time with various time intervals at a scan rate of 50 mV s^{-1}.

Fig. 9 (A) Measurements of Hg(II) on SDA/MWCNTs *via* square wave anodic stripping voltammetry with different concentrations of Hg(II) (1.3–158 µg L^{-1}) and (B) linear plot in 0.1 M NaNO$_3$ (pH 5.0); amplitude of 0.05 V.

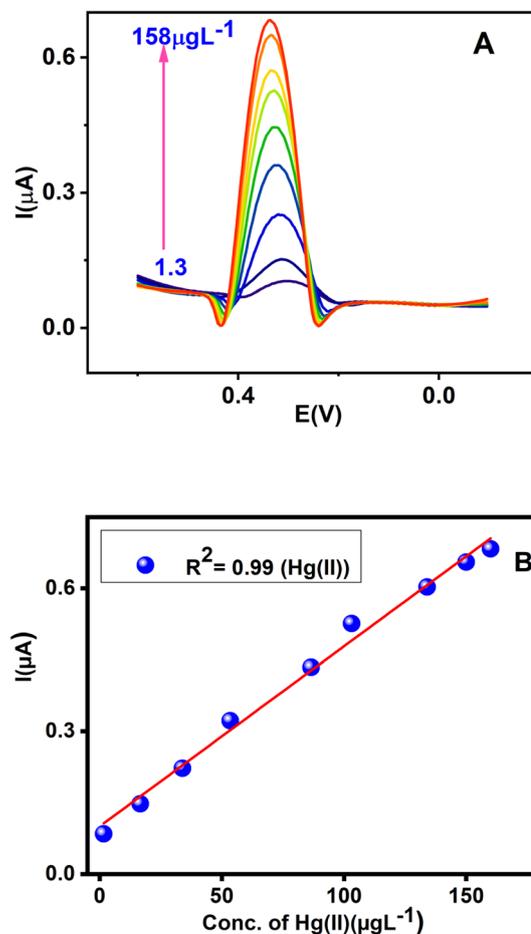observed that pH 5.0 is the most suitable pH, as the peak current for Hg(II) ion was greater at this pH. Hence, all subsequent measurements were carried out at pH 5.0.

The influence of preconcentration on the electrochemical sensing of Hg(II) was performed by SWASV. The variation in the stripping peak currents of 55 μg L^{-1} of Hg(II) in 0.1 M NaNO$_3$ was studied at different time intervals in the range from 60 to 300 s, and the results are shown in Fig. 8C. In the figure, it is clearly seen that the stripping peak current amplified sharply up to 180 s, and then decreased slightly up to 300 s. Therefore, 180 s was chosen as the optimum time for the detection of Hg(II).

3.6. Individual determination and calibration plot

The SDA/MWCNT-modified electrode was applied for different concentrations of Hg(II) from 1.3 to 158 μg L^{-1} using SWASV. The results are shown in Fig. 9A. From the figure, it was found that the stripping peak currents increase linearly with the increase in the concentration of Hg(II). A calibration graph for Hg(II) is given in Fig. 9B. A linear range was observed from 1.3 to 158 μg L^{-1} with a correlation coefficient (R^2) of 0.99 for Hg(II). It can be concluded that the increasing stripping peak current is directly proportional to the mass loading due to the binding capability of Hg(II) on the surface of SDA ligands and MWCNTs, as a tendency to enhance the stability of Hg(II) ions.

The linear regression equations for Hg(II) are expressed as follows:

$$I_P/\mu A = 0.037x + 0.101 \text{ μg L}^{-1} \text{ for Hg(II)}$$
$$\text{(sensitivity was 0.53 μA μg L}^{-1} \text{ cm}^{-2}\text{) (3)}$$

The detection limit was observed to be 0.24 μg L^{-1} for Hg(II).

Hence, a sensitive anodic stripping method was developed for the determination of Hg(II). Besides, the SDA/MWCNT-modified electrode can determine Hg(II) even at very low concentrations, which correlates well with the earlier reported modified electrodes (Table 1).

3.7. Stability and reproducibility

The reproducibility of five different SDA/MWCNT-modified electrodes was tested for the analysis of Hg(II). The electrodes are immersed in 0.1 M NaNO$_3$ at pH 5.0 for 55 μg per L Hg(II) (Fig. 10A). The RSD of electrodes was 1.7% for Hg(II), demonstrating that the five SD/MWCNT electrodes constructed exhibit good reliability and outstanding reproducibility.

The stability of the SDA/MWCNT-modified electrode was estimated by storing them at room temperature and by performing analysis of 55 μg per L Hg(II) using SWV over one weak (Fig. 10B). The stripping peak current of Hg(II) is slightly decreased, where the electrode observed 99.3% of its first peak current response with a standard deviation of 1.1%. The result confirmed the long-term stability of the proposed electrodes for electrochemical applications.

3.8. Interference analysis for Hg(II)

Using SDA/MWCNTs modified electrode, the interferences analysis of Hg(II) were correlated with various metal ions. The modified electrode was immersed in 0.1 M NaNO$_3$ containing 55 μg per L Hg(II) along with other metal ions such as Ni(II),

Table 1 Comparison of SDA/MWCNTs with previously reported works for the analysis of Hg(II)

Modified electrode	Measurement technique	Linear range (μg L^{-1})	LOD (μg L^{-1})	Reference
PG/GCE	DPASV	250–5000	32	43
GCE/poly(CoTABImPc)	SWASV	10–500	3.8	44
p-1,2-DAAQ/Au	SWV	1–50	0.2	45
TiO$_2$/Ni–NC/GCE	SWASV	1–1000	0.79	46
Mg–Al LDH (Mg–Al–TGA LDH)	SWASV	2.0–800	0.8	47
Functionalized gold nanoparticles/reduced graphene oxide	DPV	50–5000	7.5	48
GCE/rGO-SH/Au-NPs	DPV	1000–10000	240	49
TSAB/MWCNTs	SWASV	2.4–220	8	50
Poly(aniline-*co*-*o*-aminophenol) – PANOA/Au NPs	ASV	0.8–12.0	0.23	51
SDA/MWCNTs	SWASV	1.3–158	0.24	This is work

Table 2 Electrochemical parameters of MWCNTs and SDA/MWCNTs using CV and EIS

Characterization	Terms	PGE	MWCNTs	SDA/MWCNTs
CV	I_P	0.013	0.080 cm^2	0.153 cm^2
	I_{pa} (μA)	40 μA	75 μA	205 μA
	ΔE_P	267 mV	220 mV	180 mv
EIS	R_s	54.3	30.16 Ω	24.2 Ω
	R_{ct}	7370	986.2 Ω	200.4 Ω
	σ	167 × 10^{-5} S cm^{-1}	234.1 × 10^{-5} S cm^{-1}	408.1 × 10^{-5} S cm^{-1}

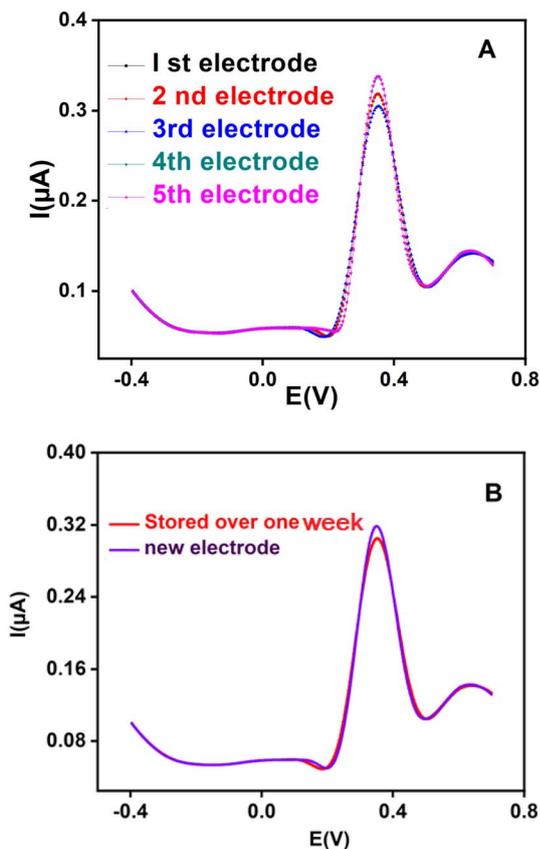© 2024 The Author(s). Published by the Royal Society of Chemistry

Fig. 10 (A) Stripping measurement of Hg(II) by reproducibility for different SDA/MWCNT electrodes and (B) stability of SDA/MWCNT electrodes containing 55 μg per L Hg(II) in 0.1 M NaNO₃.
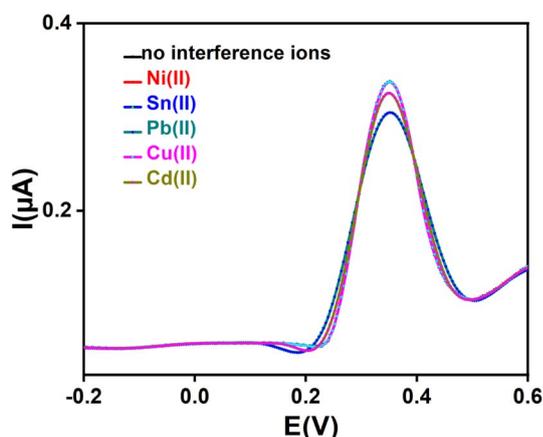

Fig. 11 Interference measurements of Hg(II) ions using SDA/MWCNTs and various metal ions (Ni(II), Sn(II), Pb(II), Cu(II) and Cd(II)) at a Hg(II) concentration of 55 μg L⁻¹ in 0.1 M NaNO₃.

Sn(II), Pb(II), Cu(II) and Cd(II) at a concentration of 55 μg L⁻¹ and optimized. The interference results are shown in Fig. 11. It implies that Sn(II), Cd(II) and Pb(II) show minimal interfering behaviour in the detection of Hg(II). The stripping peak of Hg(II) decreased in the presence of Sn(II), Cd(II) and Pb(II), as these
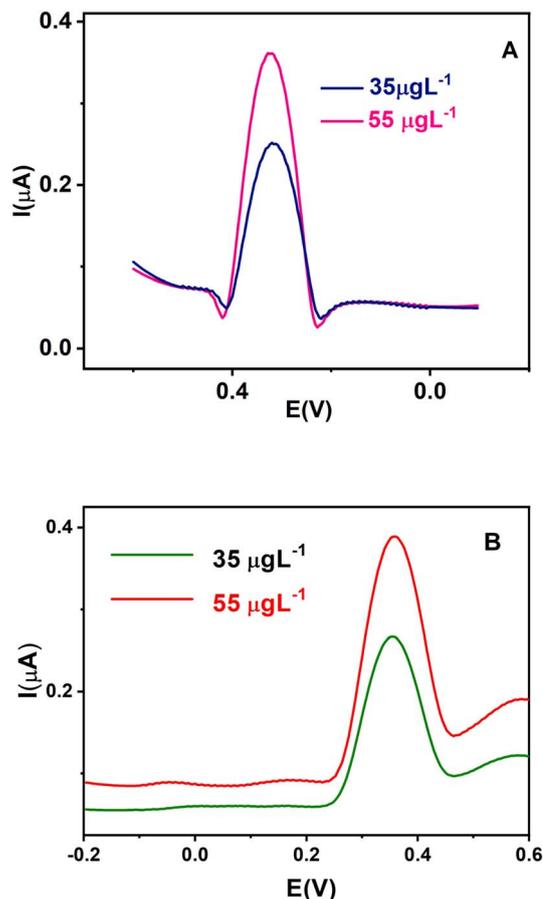

Fig. 12 SWASV studies for freshly prepared (A) chicken liver and snail shell (B) extracts at 35 and 55 μg L⁻¹ of Hg(II) in a 0.1 M NaNO₃ medium.

metal ions have the efficiency to bind at the active sites of the SDA/MWCNT-modified electrode. Furthermore, the interference of Ni(II) and Cu(II) shows no more variation in the stripping peak currents for Hg(II). Therefore, the novel proposed electrode exhibited an excellent interference study for the detection of Hg(II).

3.9. Analysis of Hg(II) in real samples

To measure the precision of the proposed sensor, Hg(II) was detected in freshly prepared chicken liver and snail shell extract samples respectively. The chicken liver and snail shell extract samples were taken from Poonamallee (Avadi), Tamil Nadu, India. The samples were diluted with 0.1 M NaNO₃ medium (pH-5.0) and the results of stripping voltammetry for Hg(II) in samples with various concentrations of chicken liver (Fig. 12A) and snail shell extract (Fig. 12B) are given. The recovery results are given in Table 3. For the samples, good recoveries (99.4 to 102.3% for Hg(II)) were observed. The result of samples were verified with those obtained by AAS. Hence, the prepared sensor showed sensible recovery for the detection of Hg(II) in different samples. It confirms that the proposed sensor shows outstanding ability for the precise detection of Hg(II) in chicken liver (sample-A) and snail shell extracts (sample-B).

Table 3 Measurement of Hg(II) in chicken liver and snail shell extract samples correlated with AAS for the analysis of Hg(II) ($n = 3$)

Samples	Metal ions	Square wave anodic stripping voltammetry (SWASV)				Atomic absorption spectroscopy (AAS)	
		Added ($\mu g\ L^{-1}$)	Found ($\mu g\ L^{-1}$)	RSD (%)	Recovery (%)	Found ($\mu g\ L^{-1}$)	Recovery (%)
Sample-A (chicken liver extract sample)	Hg(II)	35.0	34.8	1.3	99.4	35.0	100.0
		55.0	56.0	1.7	102.0	55.0	100.0
Sample-B (snail shell extract sample)	Hg(II)	35.0	35.3	2.0	101.0	35.0	102.0
		55.0	56.3	2.1	102.3	55.0	103.0

4. Conclusion

A method for the detection of Hg(II) using SDA/MWCNTs by SWASV was proposed. The SDA/MWCNTs measured Hg(II) in chicken liver and snail shell extract samples by SWASV. A good recovery from 99.4 to 102.3% was observed for Hg(II). These values were correlated with AAS. The stripping voltammetry for Hg(II) was observed in the range between 1.3 and 158 $\mu g\ L^{-1}$, with a correlation coefficient (R^2) of 0.99, an LOD of 0.24 $\mu g\ L^{-1}$ and a sensitivity of 0.53 $\mu g\ L^{-1}\ cm^2$ for Hg(II). The stability comparsion of two electrodes SDA/MWCNTs (freshly and stored for one week) modified electrodes, stripping current peak for Hg(II) was stabled. Anti-interference studies, intercorrelated with other metal ions, observed that there is no change in the stripping peak of Hg(II) with $\pm$ 5% error. Finally, the novel synthesised SDA/MWCNT electrode enhanced the sensitivity of Hg(II) effectively.

Conflicts of interest

There are no conflicts to declare.

Acknowledgements

References

1 E. G. Pacyna, J. M. Pacyna, K. Sundseth, J. Munthe, K. Kindbom, S. Wilson, F. Steenhuisen and P. Maxson, Global emission of mercury to the atmosphere from anthropogenic sources in 2005 and projections to 2020, *Atmos. Environ.*, 2010, **44**(20), 2487–2499.

2 D. Zhang, L. Wang, H. Zeng, P. Yan, J. Nie, V. K. Sharma and C. Wang, A three-dimensional macroporous network structured chitosan/cellulose biocomposite sponge for rapid and selective removal of mercury (II) ions from aqueous solution, *Chem. Eng. J.*, 2019, **363**, 192–202.

3 J. Wang and X. Qian, A series of polyamide receptor based PET fluorescent sensor molecules: positively cooperative Hg^{2+} ion binding with high sensitivity, *Org. Lett.*, 2006, **8**(17), 3721–3724.

4 M. Jaishankar, T. Tseten, N. Anbalagan, B. B. Mathew and K. N. Beeregowda, Toxicity, mechanism and health effects of some heavy metals, *Interdiscip. Toxicol.*, 2014, **7**(2), 60–72.

5 B. M. Herath, P. N. Yapa and D. M. Duminda, The Impact of the Surrounding Land Uses on Water Quality of Some Selected Cascade and Perennial Tanks in Anuradhapura District, Sri Lanka, *Turkish Journal of Agriculture-Food Science and Technology*, 2022, **10**, 3063–3069.

6 K. L. Smalling, P. M. Bradley, K. M. Romanok, S. M. Elliot, J. de Lambert, M. J. Focazio, S. E. Gordon, J. L. Gray, L. K. Kanagy, M. L. Hladik and K. A. Loftin, Exposures and potential health implications of contaminant mixtures in linked source water, finished drinking water, and tapwater from public-supply drinking water systems in Minneapolis/St. Paul area, USA, *Environ. Sci.: Water Res. Technol.*, 2023, **9**(7), 1813–1828.

7 L. T. Budnik and L. Casteleyn, Mercury pollution in modern times and its socio-medical consequences, *Sci. Total Environ.*, 2019, **654**, 720–734.

8 Y. Xin, Z. Zhou, Q. Ming, D. Sun, J. Han, X. Ye, S. Dai, L. M. Jiang, X. Zhao and Y. An, A two-stage desalination process for zero liquid discharge of flue gas desulfurization wastewater by chloride precipitation, *J. Hazard. Mater.*, 2020, **397**, 122744.

9 T. Li, T. Su, J. Wang, S. Zhu, Y. Zhang, Z. Geng, X. Wang and Y. Gao, Simultaneous removal of sulfate and nitrate from real high-salt flue gas wastewater concentrate *via* a waste heat crystallization route, *J. Cleaner Prod.*, 2023, **382**, 135262.

10 W. L. Zhang, L. Y. Zhao, Z. J. Yuan, D. Q. Li and L. Morrison, Assessment of the long-term leaching characteristics of cement-slag stabilized/solidified contaminated sediment, *Chemosphere*, 2021, **267**, 128926.

11 B. Bai, F. Bai, X. Li, Q. Nie, X. Jia and H. Wu, The remediation efficiency of heavy metal pollutants in water by industrial red mud particle waste, *Environ. Technol. Innovation*, 2022, **28**, 102944.

12 D. Ge, H. Yuan, J. Xiao and N. Zhu, Insight into the enhanced sludge dewaterability by tannic acid conditioning and pH regulation, *Sci. Total Environ.*, 2019, **679**, 298–306.

13 B. Bai, D. Rao, T. Chang and Z. Guo, A nonlinear attachment-detachment model with adsorption hysteresis for

suspension-colloidal transport in porous media, *J. Hydrol.*, 2019, **578**, 124080.

14 A. Munir, A. Shah and B. Piro, Development of a selective electrochemical sensing platform for the simultaneous detection of Tl^+, Cu^{2+}, Hg^{2+}, and Zn^{2+} ions, *J. Electrochem. Soc.*, 2018, **165**(10), B399.

15 H. B. Sonmez and N. Bicak, Quaternization of poly(4-vinyl pyridine) beads with 2-chloroacetamide for selective mercury extraction, *React. Funct. Polym.*, 2002, **51**(1), 55–60.

16 P. B. Tchounwou, C. G. Yedjou, A. K. Patlolla and D. J. Sutton, Heavy metal toxicity and the environment. Molecular, clinical and environmental toxicology, *Environ. Toxicol.*, 2012, **3**, 133–164.

17 D. Cudjoe and P. M. Acquah, Environmental impact analysis of municipal solid waste incineration in African countries, *Chemosphere*, 2021, **265**, 129186.

18 T. C. Egbosiuba, A. S. Abdulkareem, A. S. Kovo, E. A. Afolabi, J. O. Tijani and W. D. Roos, Enhanced adsorption of As(V) and Mn(VII) from industrial wastewater using multi-walled carbon nanotubes and carboxylated multi-walled carbon nanotubes, *Chemosphere*, 2020, **254**, 126780.

19 W. L. Zhang, L. Y. Zhao, Z. J. Yuan, D. Q. Li and L. Morrison, Assessment of the long-term leaching characteristics of cement-slag stabilized/solidified contaminated sediment, *Chemosphere*, 2021, **267**, 128926.

20 L. Ma, X. Zhang, M. Ikram, M. Ullah, H. Wu and K. Shi, Controllable synthesis of an intercalated ZIF-67/EG structure for the detection of ultratrace Cd^{2+}, Cu^{2+}, Hg^{2+} and Pb^{2+} ions, *Chem. Eng. J.*, 2020, **395**, 125216.

21 O. Bandeliuk, A. Assaf, M. Bittel, M. J. Durand and G. Thouand, Development and automation of a bacterial biosensor to the targeting of the pollutants toxic effects by Portable Raman Spectrometer, *Sensors*, 2022, **22**(12), 4352.

22 Q. Liang, H. Jing and D. C. Gregoire, Determination of trace elements in granites by inductively coupled plasma mass spectrometry, *Talanta*, 2000, **51**(3), 507–513.

23 M. Channegowda, Recent advances in environmentally benign hierarchical inorganic nano-adsorbents for the removal of poisonous metal ions in water: a review with mechanistic insight into toxicity and adsorption, *Nanoscale Adv.*, 2020, **2**(12), 5529–5554.

24 A. Khan, S. Malik, N. Ali, M. Bilal, Y. Yang, M. S. Akhter, C. Zhou, Y. Wenjie and H. M. Iqbal, Nanobiosorbents: Basic principles, synthesis, and application for contaminants removal, In, *Nano-Biosorbents for Decontamination of Water, Air, and Soil Pollution*, Elsevier, 2022 Jan 1, pp. 45–59.

25 M. Zaib, M. M. Athar, A. Saeed and U. Farooq, Electrochemical determination of inorganic mercury and arsenic—A review, *Biosens. Bioelectron.*, 2015, **74**, 895–908.

26 D. Martín-Yerga, M. B. González-García and A. Costa-García, Electrochemical determination of mercury: A review, *Talanta*, 2013, **116**, 1091–1104.

27 A. Shah, S. Sultan, A. Zahid, S. Aftab, J. Nisar, S. Nayab, R. Qureshi, G. S. Khan, H. Hussain and S. A. Ozkan, Highly sensitive and selective electrochemical sensor for the trace level detection of mercury and cadmium, *Electrochim. Acta*, 2017, **258**, 1397–1403.

28 Q. Lin, X. M. Jiang, X. Q. Ma, J. Liu, H. Yao, Y. M. Zhang and T. B. Wei, Novel bispillar [5] arene-based AIEgen and its' application in mercury (II) detection, *Sens. Actuators, B*, 2018, **272**, 139–145.

29 H. Karimi-Maleh, H. Beitollahi, P. S. Kumar, S. Tajik, P. M. Jahani, F. Karimi, C. Karaman, Y. Vasseghian, M. Baghayeri, J. Rouhi and P. L. Show, Recent advances in carbon nanomaterials-based electrochemical sensors for food azo dyes detection, *Food Chem. Toxicol.*, 2022, **164**, 112961.

30 Z. Li, S. Xia, J. Wang, C. Bian and J. Tong, Determination of trace mercury in water based on N-octylpyridinium ionic liquids preconcentration and stripping voltammetry, *J. Hazard. Mater.*, 2016, **301**, 206–213.

31 Y. Zhang, Y. Liu, X. Ji, C. E. Banks and W. Zhang, Sea cucumber-like hydroxyapatite: cation exchange membrane-assisted synthesis and its application in ultra-sensitive heavy metal detection, *Chem. Commun.*, 2011, **47**(14), 4126–4128.

32 M. P. Bui, J. Brockgreitens, S. Ahmed and A. Abbas, Dual detection of nitrate and mercury in water using disposable electrochemical sensors, *Biosens. Bioelectron.*, 2016, **85**, 280–286.

33 H. Karimi-Maleh, C. Karaman, O. Karaman, F. Karimi, Y. Vasseghian, L. Fu, M. Baghayeri, J. Rouhi, P. Senthil Kumar, P. L. Show and S. Rajendran, Nanochemistry approach for the fabrication of Fe and N co-decorated biomass-derived activated carbon frameworks: a promising oxygen reduction reaction electrocatalyst in neutral media, *J. Nanostruct. Chem.*, 2022, **12**(3), 429–439.

34 M. Nodehi, M. Baghayeri and H. Veisi, Preparation of GO/Fe3O4@ PMDA/AuNPs nanocomposite for simultaneous determination of As^{3+} and Cu^{2+} by stripping voltammetry, *Talanta*, 2021, **230**, 122288.

35 M. Nodehi, M. Baghayeri and H. Veisi, Preparation of GO/Fe3O4@ PMDA/AuNPs nanocomposite for simultaneous determination of As^{3+} and Cu^{2+} by stripping voltammetry, *Talanta*, 2021, **230**, 122288.

36 B. C. Janegitz, L. C. Figueiredo-Filho, L. H. Marcolino-Junior, S. P. Souza, E. R. Pereira-Filho and O. Fatibello-Filho, Development of a carbon nanotubes paste electrode modified with crosslinked chitosan for cadmium (II) and mercury (II) determination, *J. Electroanal. Chem.*, 2011, **660**(1), 209–216.

37 H. Karimi-Maleh, F. Karimi, M. Alizadeh and A. L. Sanati, Electrochemical sensors, a bright future in the fabrication of portable kits in analytical systems, *Chem. Rec.*, 2020, **20**(7), 682–692.

38 M. Baghayeri, H. Alinezhad, M. Tarahomi, M. Fayazi, M. Ghanei-Motlagh and B. Maleki, A non-enzymatic hydrogen peroxide sensor based on dendrimer functionalized magnetic graphene oxide decorated with palladium nanoparticles, *Appl. Surf. Sci.*, 2019, **478**, 87–93.

39 H. Karimi-Maleh and O. A. Arotiba, Simultaneous determination of cholesterol, ascorbic acid and uric acid

as three essential biological compounds at a carbon paste electrode modified with copper oxide decorated reduced graphene oxide nanocomposite and ionic liquid, *J. Colloid Interface Sci.*, 2020, **560**, 208–212.

40 H. Karimi-Maleh, M. Alizadeh, Y. Orooji, F. Karimi, M. Baghayeri, J. Rouhi, S. Tajik, H. Beitollahi, S. Agarwal, V. K. Gupta and S. Rajendran, Guanine-based DNA biosensor amplified with Pt/SWCNTs nanocomposite as analytical tool for nanomolar determination of daunorubicin as an anticancer drug: a docking/experimental investigation, *Ind. Eng. Chem. Res.*, 2021, **60**(2), 816–823.

41 J. Liu, B. Zhang, B. Wu, K. Zhang and S. Hu, The direct electrochemical synthesis of Ti (II), Fe (II), Cd (II), Sn (II), and Pb (II) complexes with N, N-bis (Salicylidene)-o-phenylenediamine, *Turk. J. Chem.*, 2007, **31**(6), 623–629.

42 J. Gayathri, K. S. Selvan and S. S. Narayanan, Fabrication of carbon nanotube and synthesized Octadentate ligand modified electrode for determination of Hg (II) in Sea water and Lake water using square wave anodic stripping voltammetry, *Sensing and Bio-Sensing research*, 2018, **19**, 1–6.

43 W. Yi, Z. He, J. Fei and X. He, Sensitive electrochemical sensor based on poly(L-glutamic acid)/graphene oxide composite material for simultaneous detection of heavy metal ions, *RSC Adv.*, 2019, **9**(30), 17325–17334.

44 M. Palanna, S. Aralekallu, C. K. Prabhu, V. A. Sajjan and L. K. Sannegowda, Nanomolar detection of mercury (II) using electropolymerized phthalocyanine film, *Electrochim. Acta*, 2021, **367**, 137519.

45 E. A. Shalaby, A. M. Beltagi, A. A. Hathoot and M. A. Azzem, Development of a Sensor Based on Poly(1,

2-diaminoanthraquinone) for Individual and Simultaneous Determination of Mercury (II) and Bismuth (III), *Electroanalysis*, 2022, **34**(3), 523–534.

46 X. Wang, X. Bai, W. Wang, Z. Zhao and J. Shan, TiO₂/Ni–NC Hybrid Derived from Ti₃C₂TX/NiMOF for Highly Sensitive Electrochemical Sensing of Mercury Ions, *J. Electrochem. Soc.*, 2023, **170**(3), 037519.

47 K. Asadpour-Zeynali and R. Amini, A novel voltammetric sensor for mercury (II) based on mercaptocarboxylic acid intercalated layered double hydroxide nanoparticles modified electrode, *Sens. Actuators, B*, 2017, **246**, 961–968.

48 N. Wang, M. Lin, H. Dai and H. Ma, Functionalized gold nanoparticles/reduced graphene oxide nanocomposites for ultrasensitive electrochemical sensing of mercury ions based on thymine–mercury–thymine structure, *Biosens. Bioelectron.*, 2016, **79**, 320–326.

49 N. R. Devi, M. Sasidharan and A. K. Sundramoorthy, Gold nanoparticles-thiol-functionalized reduced graphene oxide coated electrochemical sensor system for selective detection of mercury ion, *J. Electrochem. Soc.*, 2018, **165**(8), B3046–B3053.

50 J. Gayathri, K. S. Selvan and S. S. Narayanan, A novel sensor for the determination of Hg²⁺ in waters based on octadentate ligand immobilized multi-walled carbon nanotube attached to paraffin wax impregnated graphite electrodes (PIGE), *J. Solid State Electrochem.*, 2018, **22**, 2879–2888.

51 F. H. Narouei, L. Livernois, D. Andreescu and S. Andreescu, Highly sensitive mercury detection using electroactive gold-decorated polymer nanofibers, *Sens. Actuators, B*, 2021, **329**, 129267.